processes

MDPI

Article

Design of Polymer-Embedded Heterogeneous Fenton Catalysts for the Conversion of Organic Trace Compounds

Christoph Horn [1,2], Stephanie Ihmann [1,2], Felix Müller [1], Doris Pospiech [1,*], Konstantin B. L. Borchert [1,3], Rolf Hommel [4], Kaite Qin [4], Kai Licha [5], Peter J. Allertz [6] and Marco Drache [7]

1 Leibniz-Institut für Polymerforschung Dresden e.V., Hohe Str. 6, 01069 Dresden, Germany; horn-christoph@ipfdd.de (C.H.); ihmann@ipfdd.de (S.I.); muellerfelix@freenet.de (F.M.); borchert@ipfdd.de (K.B.L.B.)
2 Organic Chemistry of Polymers, Technische Universität Dresden, 01069 Dresden, Germany
3 Physical Chemistry of Polymeric Materials, Technische Universität Dresden, 01069 Dresden, Germany
4 IFN Forschungs-und Technologiezentrum GmbH, Dr.-Bergius-Str. 19, 06729 Tröglitz-Elsteraue, Germany; R.Hommel@ifn-FTZ.de (R.H.); K.Qin@ifn-FTZ.de (K.Q.)
5 FEW Chemicals GmbH, Technikumstr. 1, 06766 Bitterfeld-Wolfen, Germany; kai.licha@few.de
6 Faculty of Natural Science, Brandenburg University of Technology, Universitätsplatz 1, 01968 Senftenberg, Germany; allertz@b-tu.de
7 Institut für Technische Chemie, Technische Universität Clausthal, Arnold-Sommerfeld-Str. 4, 38678 Clausthal-Zellerfeld, Germany; marco.drache@tu-clausthal.de
* Correspondence: pospiech@ipfdd.de; Tel.: +49-351-465-8497

check for updates

Citation: Horn, C.; Ihmann, S.; Müller, F.; Pospiech, D.; Borchert, K.B.L.; Hommel, R.; Qin, K.; Licha, K.; Allertz, P.J.; Drache, M. Design of Polymer-Embedded Heterogeneous Fenton Catalysts for the Conversion of Organic Trace Compounds. *Processes* **2021**, *9*, 942. https://doi.org/10.3390/pr9060942

Academic Editors: Bipro Ranjan Dhar and Biplob Pramanik

Received: 27 April 2021
Accepted: 25 May 2021
Published: 26 May 2021

Publisher's Note: MDPI stays neutral with regard to jurisdictional claims in published maps and institutional affiliations.

Copyright: © 2021 by the authors. Licensee MDPI, Basel, Switzerland. This article is an open access article distributed under the terms and conditions of the Creative Commons Attribution (CC BY) license (https://creativecommons.org/licenses/by/4.0/).

Abstract: Advanced oxidation processes are the main way to remove persistent organic trace compounds from water. For these processes, heterogeneous Fenton catalysts with low iron leaching and high catalytic activity are required. Here, the preparation of such catalysts consisting of silica-supported iron oxide (Fe_2O_3/SiO_x) embedded in thermoplastic polymers is presented. The iron oxide catalysts are prepared by a facile sol–gel procedure followed by thermal annealing (calcination). These materials are mixed in a melt compounding process with modified polypropylenes to stabilize the Fe_2O_3 catalytic centers and to further reduce the iron leaching. The catalytic activity of the composites is analyzed by means of the *Reactive Black* 5 (RB5) assay, as well as by the conversion of phenol which is used as an example of an organic trace compound. It is demonstrated that embedding of silica-supported iron oxide in modified polypropylene turns the reaction order from pseudo-first order (found for Fe_2O_3/SiO_x catalysts), which represents a mainly homogeneous Fenton reaction, to pseudo-zeroth order in the polymer composites, indicating a mainly heterogeneous, surface-diffusion-controlled process.

Keywords: Fenton process; heterogeneous Fenton; polymer composite; degradation; iron oxide; sol–gel; trace organic compound; *Reactive Black* 5; phenol degradation

1. Introduction

Water is one of the most important resources for life on earth. The contamination of water by agricultural and industrial wastes and microplastics has become a challenging problem of today's life and inspires various research projects. Organic trace pollutants such as phenolic compounds, dyes and pharmaceuticals accumulate in surface waters due to their persistence in conventional water treatment processes. Phenolic compounds, commonly used in sectors such as oil refining, petrochemical, chemical and pharmaceutical industries and as educts for plastics, have high toxicity to humans due to their carcinogenic and mutagenic properties and are frequently found in surface and tap waters [1,2]. Synthetic dyes are widely produced and used in textile industry due to their brilliant hues, low cost and facile synthesis. More than 7×10^5 tons of synthetic dyes are produced annually and between 10 and 25% of them are lost during the dyeing process [3,4]. Many

of these dyes are classified as toxic, carcinogenic or mutagenic and cannot be removed from wastewater [5].

Conventional three-step wastewater treatment does not sufficiently remove these substances, mainly due to their chemical persistence. Therefore, more efficient methods are needed. Advanced oxidation processes (AOPs) show high efficiency in treating various persistent organic compounds due to the in situ generation of nonselective, highly reactive hydroxyl radicals, which are among the most powerful oxidizing agents. A wide range of organic compounds react with hydroxyl radicals and are converted into small organic molecules, usually CO_2 and H_2O [6–8].

The Fenton process, first observed by Henry J. Fenton [9], is considered to be one of the most effective AOPs. The conventional Fenton process proceeds in a homogeneous phase in aqueous solution. The formation of the free hydroxyl radicals occurs through decomposition of hydrogen peroxide catalyzed by dissolved Fe^{2+} ions. The traditional homogeneous process is limited by a narrow pH range, formation of iron hydroxide sludge and excessive consumption of iron and hydrogen peroxide [6,10]. Therefore, the heterogeneous Fenton process catalyzed by supported iron oxide catalysts has gained increasing attention and research activities. Its advantages include the stabilization of the iron (oxide) within the catalyst and the resolution of previous limitations in that the catalyst can continuously generate hydroxyl radicals with H_2O_2 and can also be easily removed and reused after the process [10–14]. Heterogeneous Fenton catalysts have been recently developed with different types of iron oxide, such as goethite (α-FeOOH) [15], hematite (α-Fe_2O_3) [16,17] and magnetite (Fe_3O_4) [18]. However, iron oxide based materials exhibit low surface areas and high iron leaching, which directly affects the course of the heterogeneous Fenton reaction [11]. The incorporation in or immobilization of iron-containing materials on various supports, such as microporous zeolites and mesostructured silica materials, resulted in materials with reduced iron leaching, higher stability and higher surface area [19–23]. Nevertheless, zeolites and mesostructured silica materials are costly because of the necessity to use structure formers or highly reactive silica sources (silanes), which has limited the application in industry up to the present. Recently, Martínez et al. [24] reported low-cost heterogeneous silica-supported iron catalysts for industrial Fenton applications prepared by a simple sol–gel synthesis route. The catalysts prepared with tetraethyl orthosilicate (TEOS) showed high activities but still exhibited iron leaching, which is unfavorable in wastewater treatment processes.

The aim of the study presented here was to prepare low-cost heterogeneous Fe_2O_3/SiO_x-based Fenton catalysts with improved properties, in particular with reduced iron leaching, for the degradation of trace organic compounds in water. The Fenton catalysts were prepared based on the procedure of Martínez et al. [24] with slight variations. Embedding the catalysts in a polymer matrix was employed for a further drastic reduction in iron leaching and to enhance the mechanical stability of the catalysts required under the harsh conditions in wastewater treatment. To the best of our knowledge, embedding Fenton catalysts into thermoplastic polymers has not yet been reported. Application of thermoplastic polymer matrices enabled the use of melt processing procedures for the preparation of the final composite. The concept is outlined in Scheme 1.

The Fe_2O_3/SiO_x catalysts were analyzed by X-ray diffraction (XRD) and X-ray fluorescence (XRF) analysis and nitrogen (N_2) sorption to determine their composition, chemical structure and surface area. Furthermore, the catalytic activity was analyzed using the *Reactive Black* 5 (RB5) assay as well as the reaction with phenol. After these analyses, the Fe_2O_3/SiO_x materials were embedded in thermoplastic polymers by melt compounding. Polypropylenes with varied polarity (polypropylene, maleic anhydride grafted polypropylene, and maleic anhydride grafted polypropylene further reacted with different poly(alkylene oxide)s) were selected to understand the influence of polarity.

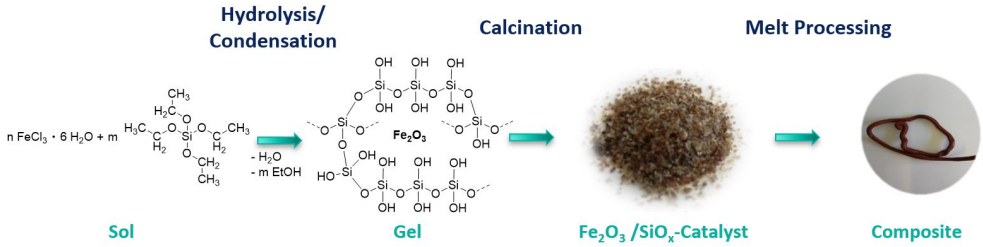

Scheme 1. Schematic presentation of the preparation of low-cost Fe_2O_3/SiO_x Fenton catalysts by embedding the thermally treated sol–gel materials into a thermoplastic matrix resulting in composites.

The Fenton polymer composites were again analyzed by the RB5 assay and by phenol degradation. In both processes, the leaching of iron species was simultaneously monitored by inductively coupled plasma optical emission spectroscopy (ICP-OES). Furthermore, the kinetics of the RB5 degradation were followed by time-dependent measurements. These studies should provide clear evidence of whether the catalyst composites allow a heterogeneous Fenton process. In addition, degradation studies of organic compounds catalyzed by the composites were performed. The residual concentration of organic trace compounds belonging to different classes was monitored: diclofenac (DFC) as analgesic, 17α-ethinylestradiol (EED) as contraceptive, *p*-chlorophenol (*p*CP) as herbicide and fungicide and bisphenol A (BPA) as base material and softener of polymers. These different compounds should allow the evaluation of the potential of the Fenton catalysts.

2. Materials and Methods

2.1. Materials

(3-Aminopropyl)triethoxysilane (APTES, 99%, Sigma-Aldrich Chemie GmbH, Munich, Germany), ammonia solution (NH_3, 30%, Carl Roth GmbH, Karlsruhe, Germany) 2,2-bis-(4-hydroxyphenyl)-propane (bisphenol A, BPA, ≥99%, Sigma-Aldrich Chemie GmbH, Munich, Germany), 2-{2-[(2,6-dichloro-phenyl)amino]phenyl}ethanoic acid dinatrium salt (diclofenac, DFC, ≥98%, Sigma-Aldrich Chemie GmbH, Munich, Germany), ethanol (EtOH, 96%, BCD Chemie GmbH, Hildesheim, Germany), 17α-ethinylestradiol (EED, ≥98%, Sigma-Aldrich Chemie GmbH, Munich, Germany), hydrochloric acid (HCl, 1 mol/L, Carl Roth GmbH, Karlsruhe, Germany), hydrogen peroxide (H_2O_2, 30%, Carl Roth GmbH, Karlsruhe, Germany), iron(III) chloride hexahydrate ($FeCl_3 \times 6\ H_2O$, ≥98%, Carl Roth GmbH, Karlsruhe, Germany), nitric acid (HNO_3, 65%, Sigma-Aldrich Chemie GmbH, Munich, Germany), *p*-chlorophenol (*p*CP, ≥99%, Sigma-Aldrich Chemie GmbH, Munich, Germany), phenol (≥99%, Sigma-Aldrich Chemie GmbH, Munich, Germany), *Reactive Black* 5 (RB5, ≥50%, Sigma-Aldrich Chemie GmbH, Munich, Germany), poly(ethylene oxide-*co*-propylene oxide)-monoamine (P(EO-*co*-PO)-$NH_{2\text{-}600}$, Jeffamine M-600, M_n = 600 g/mol, Huntsman Corporation, Salt Lake City, UT, USA), poly(ethylene oxide-*co*-propylene oxide)-monoamine (P(EO-*co*-PO)-$NH_{2\text{–}1000}$, Jeffamine M-1000, M_n = 1000 g/mol, Huntsman Corporation, Salt Lake City, UT, USA), poly(propylene-*g*-maleic anhydride) (PP-*g*-MA, Exxelor PO 1020, M_w = 23,000 g/mol, ExxonMobile, Irving, TX, USA) and tetraethoxysilane (XIAMETER OFS-6697, ≥99%, Dow Silicones Deutschland GmbH, Wiesbaden, Germany) were used as received.

2.2. Procedures

2.2.1. Synthesis of the Fe_2O_3/SiO_x Fenton Catalysts F1 and F2

To a mixture of 300 mL ethanol and 140 mL deionized water, $FeCl_3 \times 6\ H_2O$ (20.00 g, 0.074 mol) was added in portions under vigorous stirring. Then, tetraethoxysilane (150 g, 0.721 mol) was added, the mixture was stirred for 3 h at room temperature, followed by standing for an additional 24 h. To this precondensate, 100 mL of a 5 wt.% ammonia solution was added under stirring, thereby converting the mixture into a viscous gelled material. The mixture was placed on filter paper to dry in air for four days. Subsequently, the material was dried for 4 h at 150 °C in an oven, followed by calcination at 550 °C for

2 h (once for F1 and twice for F2), as shown in Table 1. The products were obtained as reddish-brown solid (180 g) with 20 wt.% residual solvent content.

Table 1. Characteristics of the Fe_2O_3/SiO_x catalysts obtained by sol–gel preparation followed by thermal treatment (calcination) and control samples.

Sample	Composition	Calcination	Iron Content (wt.%) [(a)]	Shape, Ø (mm)
Fe_2O_3	Fe_2O_3	-	-	Powder, 0.2
F1	Fe_2O_3/SiO_x	550 °C	6.9	Powder, 0.2
F2	Fe_2O_3/SiO_x	2 × 550 °C	7.4	Powder, 0.2

[(a)] Determined by XRF.

2.2.2. Fe_2O_3/SiO_x Polymer Composites

Polymer composites were prepared on an XPlore MC 15 Micro Compounder (Xplore/DSM, Sittard, the Netherlands). Both PP-*g*-MA and Fe_2O_3/SiO_x were predried under reduced pressure at 80 °C for 5 h in a vacuum oven. Polymer granulates (9.75 g) and Fe_2O_3/SiOx powder (5.25 g) were mixed, and the mixture was fed continuously into a filling nozzle of the micro compounder preheated to 180 °C with rotating screws (100 rpm). Mixing was carried out for five minutes. The micro compounder was then stopped, and the composite (wt.%/wt.% = 80/20 or 65/35) emerged as a strand that was ground into the desired particle size.

In addition to these experiments, reactive extrusions were performed adding (3-aminopropyl)triethoxysilane (APTES) and/or poly(ethylene oxide-*co*-propylene oxide)-monoamines (P(EO-*co*-PO)-NH_2). P(EO-*co*-PO)-NH_2 was dried over activated molar sieves (4 Å, Merck KGaA, Darmstadt, Germany) for 24 h at 80 °C. APTES was used as received. The calculated amounts of the respective P(EO-*co*-PO)-NH_2 and/or APTES were added dropwise to the predried Fe_2O_3/SiO_x, tightly sealed and stored for 24 h at room temperature. After that time, the reactive compounding was performed as described above. The detailed compositions are summarized in Table 2.

Table 2. Composition and characteristics of the Fenton polymer composites.

Sample	Polymer	Catalyst	Composition Polymer/Catalyst (wt.%/wt.%)	Shape, Ø (mm)	Pore Diameter Ø (μm) [(a)]
PP-*g*-MA/F1 (80/20)-G	PP-*g*-MA	F1	80/20	Granules, 3.1	3.1
PP-*g*-MA/F1 (80/20)-C	PP-*g*-MA	F1	80/20	Crushed, 0.9	not det.
PP-*g*-MA/F1 (80/20)	PP-*g*-MA	F1	80/20	Powder 0.2	not det.
PP-*g*-MA/F2 (65/35)	PP-*g*-MA	F2	65/35	Powder 0.2	3.2
PP-*g*-MA/APTES/F2 (65/35)	PP-*g*-MA + APTES	F2	65/35 + 1.17 APTES	Powder 0.2	1.9
PP-*g*-MA-*g*-PEO600/APTES/F2 (65/35)	PP-*g*-MA-*g*-PEO600 + APTES	F2	65/35 + 1.17 APTES	Powder 0.2	2.0
PP-*g*-MA-*g*-PEO1000/APTES/F2 (65/35)	PP-*g*-MA-*g*-PEO1000 + APTES	F2	65/35 + 1.17 APTES	Powder 0.2	0.9

[(a)] Determined by SEM; not det.: not determined.

2.3. Methods

2.3.1. X-ray Fluorescence Spectroscopy (XRF)

X-ray fluorescence spectroscopy (XRF) was carried out to determine the iron content of the Fenton catalysts by means of a Spectro XRP Analyzer Pro XEPOS C. XRF-spectrometer (SPECTRO Analytical Instruments GmbH, Kleve, Germany) (tube: voltage 45.1 kV, average current 0.887 mA; atmosphere: helium (flow rate 40 L/h); temperature: −30 °C; duration: 240 s; calibration: system-specific fundamental data from the manufacturer). Analysis of data was performed with the integrated instrument software XRF Analyzer Pro. Samples were prepared by grinding. Measurement was performed with finely ground powders in cuvettes (diameter 32 mm) with two clamping rings (Chemplex Ind., Inc., Palm City, FL, USA) terminated at the bottom by a Prolene X-ray film (thickness 4 µm, Chemplex Ind., Inc., Palm City, FL, USA). Powdered samples (sample quantity > 1 g) were positioned on Prolene X-ray films.

2.3.2. Wide-Angle X-ray Scattering (WAXS)

Wide-angle X-ray scattering (WAXS) was carried out using a 2-circle diffractometer XRD 3003 T/T (GE Sensing & Inspection Technologies, Ahrensburg, Germany) in symmetric step-scan mode with $\Delta 2\theta = 2°$ in the range of 2θ 3–66° and $t = 40$ s (using 40 kV/30 mA CuKα radiation $\lambda = 0.1542$ nm, monochromatized by primary multilayer system and slit geometry 0.2 mm 0.3 mm^{-1}). Scattering results were presented as I versus 2θ with vertically shifted curves for better visualization. All diffractograms were normalized to the main reflection of hematite at $2\theta = 33.2$ ° for better comparison.

2.3.3. Nitrogen Sorption Measurements

Nitrogen (N_2) sorption measurements were performed using an Autosorb iQ MP (Quantachrome Instruments, Boynton Beach, FL, USA). Samples were activated by degassing in vacuum (5×10^{-10} mbar) at 110 °C for 48 h. Nitrogen sorption measurements were carried out at 77 K. Surface area was calculated in the relative pressure (p/p_0) range from 0.10 to 0.25 by BET method [25]. For the derivation of the pore size distribution (PSD), NLDFT model fit for cylindrical and sphere pores for the adsorption of N_2 on silica was chosen.

2.3.4. Scanning Electron Microscope

The scanning electron microscope (SEM) Ultra plus (Carl Zeiss NTS, Jena, Germany) equipped with detector S2 was used to image surfaces of both powdered and crushed samples (Fe_2O_3/SiO_x catalysts and composites) as well as strands of extruded composite samples. An acceleration voltage of 3 keV and an aperture size of 30 mm were applied. The samples were prepared by gluing on a standard aluminum substrate followed by sputtering with 3 nm platinum films.

2.3.5. Degradation Kinetics of Reactive Black 5 (RB5)

The catalytic activity of Fenton catalysts was determined by the RB5 assay using UV/VIS spectrophotometer (SPECORD 210 PLUS, Analytik Jena GmbH, Jena, Germany). Therefore, 50 mL of a reaction solution containing RB5 (40 mg/L, 0.04 mmol/L) and H_2O_2 (200 mg/L, 6 mmol/L) was prepared in a reaction vessel, adjusted to pH 3.5 using 0.1 M HCl and stirred for homogeneous distribution. Subsequently, the Fenton catalyst was added to the stirred solution at a concentration normalized to 100 mg/L iron content in the sample. Aliquots were withdrawn during reaction course every 15 min for UV/VIS measurement and transferred through a syringe filter (Rotilabo syringe filter PTFE, pore size 0.20 µm, Carl Roth GmbH, Karlsruhe, Germany) into a cuvette (BRAND, semi-micro, PMMA, 1.5 mL). UV/VIS measurements started by adding the Fenton catalyst to the reaction solution. The change in absorbance was measured at 598 nm against a blank cuvette over a period of 120 min.

The reaction rate and reaction order of the catalytic reactions were determined using the linearization of the conversion–time curves. The validity of the reaction order obtained from the experimental data was checked by the coefficient of reliability (R^2).

The influence of radical scavengers on the degradation of RB5 was investigated by adding $O_2^{\bullet -}$ (chloroform) and $OH^{\bullet}$ (*t*-butanol) radical scavengers. The scavengers were added to the RB5 assay prior to H_2O_2 in the molar ratios of scavenger/RB5 of 50:1 and 100:1. The RB5 assay was carried out as described above.

2.3.6. Analysis of the Degradation of Phenol

Degradation studies of phenol catalyzed by the respective Fenton catalysts were carried out. First, 50 mL of a reaction solution containing phenol (100 mg/L) and H_2O_2 (200 mg/L) was prepared in a reaction vessel, adjusted to pH 3.5 using 0.1 M HCl and shaken for equal distribution. The Fenton catalyst was added subsequently to the stirred solution at a concentration normalized to 100 mg/L iron content in the sample. Aliquots were withdrawn during reaction course at selected reaction times and filtered (Rotilabo syringe filter PTFE, pore size 0.45 µm, Carl Roth GmbH, Karlsruhe, Germany) prior to analysis. The phenol concentration was followed by high-performance liquid chromatography (HPLC) technique (HPLC System 325, Kontron Instruments GmbH, Milan, Italy) equipped with a Zorbax Eclipse PHA column (diameter 3 mm, length 250 mm, pore size 5 µm; Agilent Technologies Inc., Santa Clara, CA, USA) and UV/VIS detector (UV/VIS Detector 332, Kontron Instruments GmbH, Milan, Italy) at 285 nm. A mixture of water (40 vol.%) and acetonitrile (60 vol.%) was used as mobile phase at a flow rate of 0.8 mL/min. The calibration of the equipment for above-mentioned compounds was carried out plotting the detector response as a function of analyte concentration, using a series of standards of known concentrations.

2.3.7. Iron Leaching Studies

ICP-OES (iCAP 7400, Thermo Fisher Scientific GmbH, Dreieich, Germany) was used to measure iron leaching of the Fenton catalysts. An aqueous solution (10 mL) consisting of 100 mg/L iron content in the sample with 200 mg/L H_2O_2 was prepared, adjusted to pH 3.5 by adding 0.1 M HCl and stirred for 2 h. Then, the solution was filtered through a syringe filter (0.2 µm) and heated to evaporate residual H_2O_2. To each sample of 8 mL, 2 mL 20 % HNO_3, was added prior to analysis. Ten standards were used for measurements: Standard 1: Fe (100 mg/L), Standard 2: Fe (50 mg/L), Standard 3: Fe (10 mg/L), Standard 4: Fe (5 mg/L), Standard 5: Fe (1 mg/L), Standard 6: Fe (0.5 mg/L), Standard 7: Fe (0.1 mg/L), Standard 8: Fe (0.05 mg/L), Standard 9: Fe (0.01 mg/L), Standard 10: Fe (0.005 mg/L), concentrations in 4 wt.% HNO_3. For the preparation of the standard solutions, 10,000 mg/L Fe in 2 mol/L HNO_3 (Bernd Kraft, Duisburg, Germany) was used. The concentration was determined three times and the results were averaged. The lower limit of quantification (LLOQ) of the method was <0.005 mg/L.

2.3.8. Degradation of Organic Trace Compounds

Degradation studies of organic compounds were performed with the heterogeneous Fenton catalyst F2. The residual concentration of each of the organic water pollutants DFC, BPA, *p*CP and EED used in a starting concentration of 10 µM in water was monitored at room temperature in citrate buffer (0.1 M, pH 4.5), as well as in H_2O (pH 7), after 24 h. Liquid chromatography coupled with mass spectroscopy (Agilent Triple Quadrupole LC-MS/MS 6400 system with ESI ionization, Santa Clara, CA, USA) was used to quantify the concentrations.

A solution of F2 (50 mg) in 5 mL of the corresponding organic pollutant solution (10 µM in the desired solvent—H_2O or citrate buffer) with 1 drop HCl (1 wt.%) and 100 µL H_2O_2 (33 wt.%) was prepared. Tubes were incubated under slow shaking for 24 h. The resulting mixtures were analyzed using liquid chromatography with a reversed-phase column (Phenomenex Gemini-NX 3 mm, C18, 110 Å, 100 × 2 mm, Torrance, CA, USA)

using a mixture of acetonitrile and 0.05 vol.% aqueous NH_3 solution as mobile phase. Retention times were 0.9 min for DFC, 1.30 min for *p*CP, 2.40 min for BPA and 2.80 min for EED. The separated compounds were subsequently analyzed by triple-quadrupole mass spectrometry in multiple reaction monitoring (MRM) mode. Quantifiers (126.5 for *p*CP, 145 for EED, 212 for BPA and 250 for DFC) and qualifiers were identified with ESI ionization in negative ion mode. BPA-d16 was used as internal standard for quantification and added directly before the measurement. The obtained concentration was detected after 24 h and compared to blanks. All degradation experiments were performed at least three times and the results were averaged.

3. Results and Discussion

3.1. Characterization of the Fenton Catalysts F1 and F2

Fe_2O_3/SiO_x catalysts F1 and F2 were prepared by a sol–gel method and characterized by XRD, XRF and N_2 sorption to obtain information about the iron species present, the iron content and the surface area. The influence of a double calcination procedure at 550 °C for F2 on the degradation activity and the iron leaching was studied. Iron contents of 6.9 wt.% for F1 and 7.4 wt.% for F2 were determined by XRF (Table 1). The XRD pattern (see Supplementary Material (SM), Figure S1) of powdered catalysts F1 and F2 showed characteristic diffraction reflections of crystalline hematite Fe_2O_3, while characteristic reflections of magnetite Fe_3O_4 were not observed. N_2 sorption measurements (see SM, Figure S2) revealed an increase in the surface area compared to Fe_2O_3, which indicates a mesoporous structure caused by the simultaneous formation of SiO_2 and Fe_2O_3. Values obtained for specific surface area, pore volume and micropore volume are presented in Table 3. The results proved the success of the sol–gel process and are in agreement with previous studies reported in the literature [24]. F2 showed an increase in pore volume and broadening of pores in the pore size distribution (see SM, Figure S3), presumably caused by the double calcination. However, the micropore volume (MPV) remained constant.

Table 3. Specific surface area (S_{BET}), pore volume (PV) and micropore volume (MPV) of the samples Fe_2O_3, F1 and F2.

Sample	S_{BET} (m^2 g^{-1}) [(a)]	PV (cm^3 g^{-1}) [(b)]	MPV (cm^3 g^{-1}) [(c)]
F_2O_3	5	<0.01	n.a.
F1	272	0.46	0.10
F2	264	0.69	0.10

[(a)] Surface area calculated from N_2 adsorption isotherm using multipoint BET method with $0.1 \leq p/p_0 \leq 0.25$ [25,26]. [(b)] Pore volume (PV) calculated from N_2 uptake at $p/p_0 = 0.95$, adsorption curve. [(c)] Micropore volume (MPV) calculated from N_2 uptake at $p/p_0 = 0.10$.

Determination of catalytic activity, reaction order and reaction rate coefficients by the RB5 assay is essential to evaluate the action of the catalyst (either homogeneous or heterogeneous). The azo dye RB5, characterized by the presence of an unsaturated group (–N=N–) responsible for the color, was chosen as a model substance. UV/VIS spectroscopy was used to monitor the decolorization of RB5 over a period of 120 min. Linearization of the conversion–time curves may provide information about the reaction order and the reaction rate coefficients (from the gradient of the curve). In addition, the iron leaching under Fenton conditions was analyzed, taking samples at the end of the reaction after 120 min. Significant iron leaching would indicate the occurrence of homogeneous processes in the Fenton reaction [11].

The kinetics of the heterogeneous Fenton process has been described by a "two-step kinetic model" by some authors. In the first step, an abrupt drop of RB5 intensity within 0.1 min was described (called "seconds stage"); this was followed by a stage with a steady but slower decrease (called "minutes stage") [27–29]. Covinich et al. [29] reported a heterogeneous $CuO/\gamma\text{-}Al_2O_3$ Fenton catalyst that was characterized by pseudo-zeroth-order kinetics in the "minutes stage". This kinetic model was also applied in previous

studies for the saturation step of the catalyst surface by the reactants [30]. The global kinetics were presented as follows:

$$-\frac{dC}{dt} = r = k_{OH}[HO] = k \quad (1)$$

where C represents the concentration of RB5, t is the reaction time, r is the reaction rate, k_{OH} is the kinetic reaction rate coefficient and k is the apparent pseudo-zeroth-order kinetic constant. In Figure 1, conversion–time curves of RB5 for the Fenton catalysts F1 and F2 and Fe_2O_3 (hematite) are compared. The conversions after 120 min, the calculated kinetic parameters and the iron leaching of the catalysts at t = 120 min are given in Table 4.

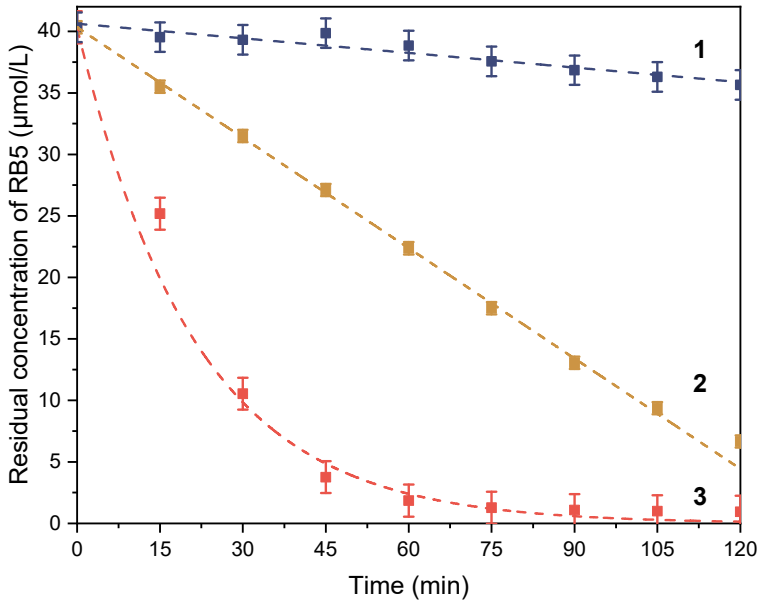

Figure 1. Degradation kinetics of RB5 using (**1**) Fe_2O_3 (hematite), (**2**) F2 and (**3**) F1 as catalysts.

Both Fe_2O_3/SiO_2 catalysts enhanced the degradation reaction of RB5 under Fenton conditions compared to conventional Fe_2O_3. This is attributed to the higher surface area caused by the mesoporous structure of SiO_2 that was formed in the coreaction of TEOS and the iron compounds. Fe_2O_3 showed a conversion of only 12% after 120 min, while 98% of RB5 could be converted by F1 and 84% of RB5 could be converted by F2. For F2, a uniform linear decrease in RB5 concentration was observed, accompanied by a weak iron leaching of < 0.1 wt.% (0.09 mg/L). The conversion–time curve could be fitted to a pseudo-zeroth-order kinetic model (with R^2 = 0.999). In contrast, the curve obtained with the F1 catalyst exhibited an exponential decrease with a 7-fold higher iron leaching and could be assigned to a pseudo-first-order kinetic model (R^2 = 0.983). A comparable behavior was reported in the literature and is indicative of a heterogeneous catalysis process for F2, while F1 predominantly catalyzed a homogeneous Fenton process [27–31].

Table 4. Kinetic parameters of the RB5 assay and iron leaching of Fe_2O_3 and the Fenton catalysts F1 and F2.

Sample	Conversion (%) [(a,b)]	Iron Leaching After 2 h [(a,c)] (mg/L)	Pseudo-Reaction Order [(a)]	Reaction Rate Coefficient [(a)]	R^2
Fe_2O_3	12	0.01	First	2.12×10^{-05} s^{-1}	0.937
F1	98	0.66	First	7.81×10^{-04} s^{-1}	0.983
F2	84	0.09	Zeroth	4.99×10^{-09} $mol \cdot L^{-1} \cdot s^{-1}$	0.999

[(a)] Iron content of all samples used was 100 mg/L, [(b)] conversion after 2 h in RB5 assay, [(c)] determined by ICP-OES.

It is known that H_2O_2 can generate $O_2^{\bullet-}$ radicals in addition to hydroxyl radicals during the Fenton reaction. To determine the influence of $O_2^{\bullet-}$ and $OH^{\bullet}$ on RB5 degradation, degradation studies of RB5 catalyzed by F2 with and without chloroform or *t*-butanol in the scavenger/RB5 molar ratios of 50:1 and 100:1 were carried out (see SM, Figure S4). Chloroform has been widely used as a scavenger of $O_2^{\bullet-}$, while *t*-butanol has been used as a scavenger of $OH^{\bullet}$ [32–34]. No significant influence of $O_2^{\bullet-}$ on the RB5 degradation could be observed for both molar ratios of chloroform to RB5 (50:1, 100:1) (see SM, Figure S4a). The degradation efficiency after 60 min decreased by 23% for a *t*-butanol to RB5 molar ratio of 50:1 and by 48% for the molar ratio 100:1 when *t*-butanol was used as $OH^{\bullet}$ scavenger. These results indicated indirectly that RB5 was oxidatively degraded mainly by $OH^{\bullet}$ radicals.

3.2. Preparation and Characterization of the Fenton Polymer Composites

3.2.1. Preparation of the Fenton Polymer Composites

To reduce iron leaching and associated homogeneous contributions during the Fenton process, the iron catalysts F1 and F2 were embedded in polymer matrices by melt processing. Maleic anhydride grafted poly(propylene) (PP-*g*-MA) was selected as a polymer. Furthermore, modification of PP-*g*-MA by reactive extrusion with poly(ethylene oxide-*co*-propylene oxide)-amine (P(EO-*co*-PO)-NH_2) (see Figure 2) of different molar masses was carried out to investigate the influence of hydrophilicity on the Fenton activity and iron leaching. Designations and compositions of the polymer composites are listed in Table 2.

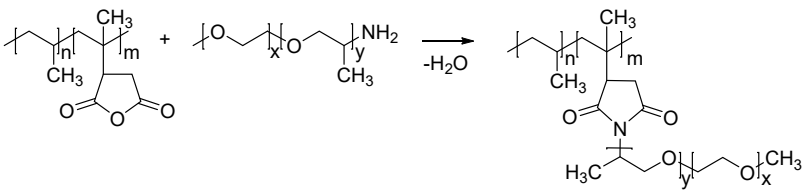

Figure 2. Reaction scheme of the reactive extrusion of PP-g-MA with P(EO-co-PO)-NH_2.

3.2.2. Catalytic Activity of the Polymer Composites as Studied by the RB5 Assay

To investigate the influence of surface area on the degradation of RB5, the polymer composites were ground and divided into three fractions (see Figure 3A–C). Scanning electron micrographs revealed an increase in roughness with the reduction in particle size.

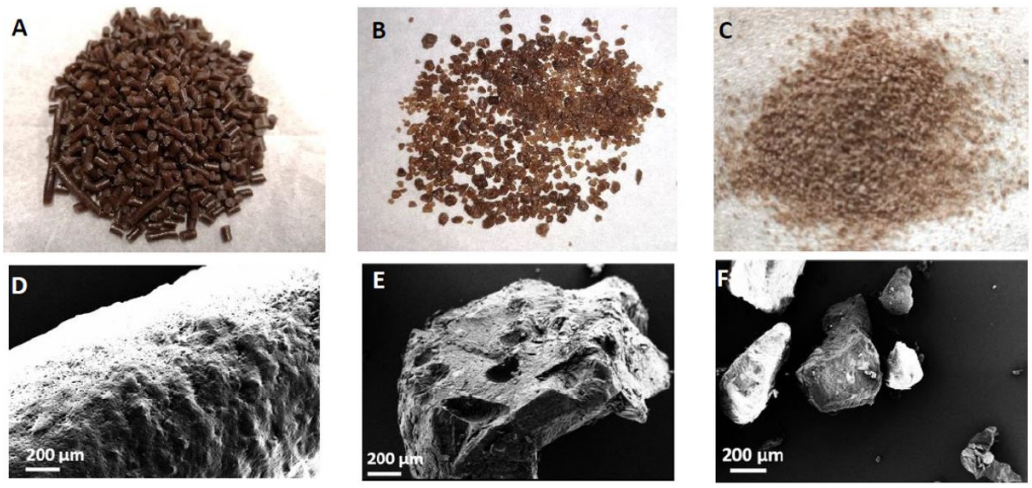

Figure 3. *Cont.*

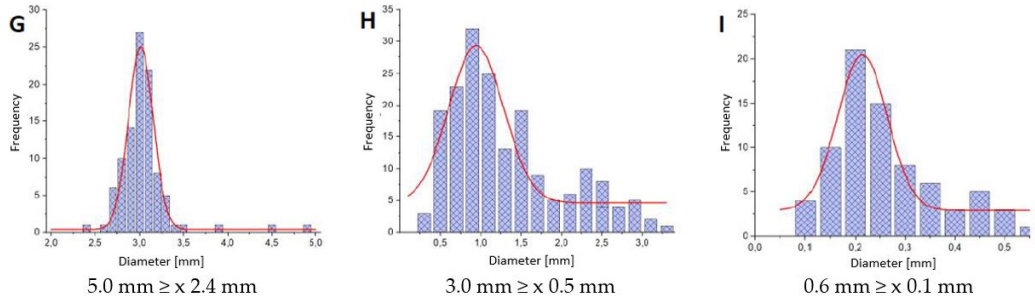

Figure 3. Photographic images of (**A**) PP-*g*-MA/F1 (80/20)-G (granules), (**B**) PP-*g*-MA/F1 (80/20)-C (crushed) and (**C**) PP-*g*-MA/F1 (80/20) (powder); SEM images of (**D**) PP-*g*-MA/F1 (80/20)-G, (**E**) PP-*g*-MA/F1 (80/20)-C and (**F**) PP-*g*-MA/F1 (80/20); and particle size distribution of (**G**) the pellet diameter of PP-*g*-MA/F1 (80/20)-G, (**H**) particle size of PP-*g*-MA/F1 (80/20)-C and (**I**) particle size of PP-*g*-MA/F1 (80/20).

Table 5 summarizes the kinetic parameters determined from conversion–time curves and the conversions of RB5 after 120 min catalysis by Fenton polymer composites. The conversion–time curves of the differently crushed PP-*g*-MA/F1 composites showed a linear progression in contrast to F1, which exhibited an exponential drop (Figure 4). Accordingly, the iron leaching of PP-*g*-MA/F1 composites was drastically reduced compared to F1.

Table 5. Kinetic parameters of the RB5 conversion catalyzed by Fenton polymer composites and iron leaching after 120 min.

Sample	RB5 Conversion (%) [(a,b)]	Iron Leaching after 2 h (mg/L) [(a,c)]	Reaction Order [(a)]	Reaction Rate Coefficient [(a)]	R^2
Fe_2O_3	12	0.01	First	2.12×10^{-05} s^{-1}	0.937
F1	98	0.66	First	7.81×10^{-04} s^{-1}	0.983
F2	85	0.09	Zeroth	4.99×10^{-09} $mol{\cdot}L^{-1}{\cdot}s^{-1}$	0.999
PP-*g*-MA/F1 (80/20)-G	7	0.04	Zeroth	3.39×10^{-10} $mol{\cdot}L^{-1}{\cdot}s^{-1}$	0.885
PP-*g*-MA/F1 (80/20)-C	16	0.04	Zeroth	8.05×10^{-10} $mol{\cdot}L^{-1}{\cdot}s^{-1}$	0.961
PP-*g*-MA/F1 (80/20)	41	0.18	Zeroth	2.17×10^{-10} $mol{\cdot}L^{-1}{\cdot}s^{-1}$	0.973
PP-*g*-MA/F2 (65/35)	19	n.d.	Zeroth	7.37×10^{-10} $mol{\cdot}L^{-1}{\cdot}s^{-1}$	0.987
PP-*g*-MA/APTES/F2 (65/35)	5	n.d.	Zeroth	2.60×10^{-10} $mol{\cdot}L^{-1}{\cdot}s^{-1}$	0.978
PP-*g*-MA-*g*-PEO600/ APTES/F2 (65/35)	17	n.d.	Zeroth	5.84×10^{-10} $mol{\cdot}L^{-1}{\cdot}s^{-1}$	0.959
PP-*g*-MA-*g*-PEO1000/ APTES/F2 (65/35)	30	0.02	Zeroth	1.03×10^{-09} $mol{\cdot}L^{-1}{\cdot}s^{-1}$	0.915

[(a)] Iron content of all samples used was 100 mg/L, [(b)] conversion after 2 h in RB5 assay, [(c)] determined by ICP-OES., n.d.: not detectable as under LLOQ.

The results obtained with the Fenton polymer composites with different particle sizes clearly showed the influence of the surface area on the kinetics, as can be expected for a surface-controlled heterogeneous Fenton process. The conversion of RB5 increased from 7% for PP-*g*-MA/F1 (80/20)-G (Ø = 3.0 mm) up to 41% for the powdered PP-*g*-MA/F1 (80/20) (Ø = 0.2 mm). Interestingly, the reaction rate coefficient of PP-*g*-MA/F1 (80/20) was lower compared to PP-*g*-MA/F1 (80/20)-G. The higher conversion was probably caused by the abrupt decrease in RB5 concentration during the "seconds stage" process. Due to the greater availability of active sites, which is significantly influenced by the surface area, $OH^{\bullet}$ radical production and oxidation of RB5 occurred rapidly. After that process, saturation of the reaction occurs in the pores, and the reaction subsequently proceeds slowly and linearly. Moreover, PP-*g*-MA/F1 (80/20) exhibited 4.5-fold higher leaching compared to PP-*g*-MA/F1 (80/20)-G, suggesting additional homogeneous contributions after the composites were ground to a powder. As a result of the high conversion, the linear curve of the RB5 degradation and the low iron leaching compared to the pure Fenton catalysts F1 and F2, all polymer composites were later ground prior to the degradation studies.

Moreover, only polymer composites with the catalyst F2 were used in the following studies, since iron leaching could be reduced by 86% through double calcination of F2.

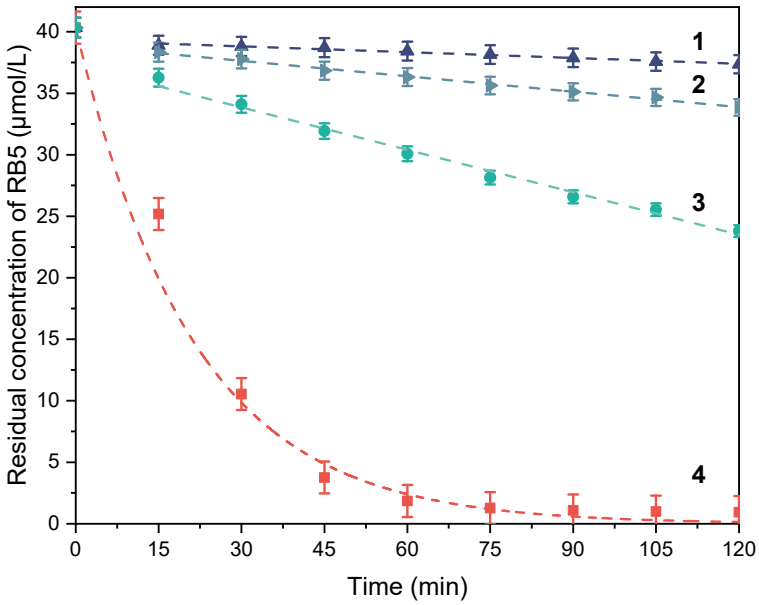

Figure 4. Degradation kinetics of RB5 catalyzed by Fenton polymer composite PP-*g*-MA/F1 (80/20) with different particle sizes: (**1**) PP-*g*-MA/F1 (80/20)-G granules with Ø = 3.1 mm, (**2**) PP-*g*-MA/F1 (80/20)-C crushed with Ø = 0.9 mm, (**3**) PP-*g*-MA/F1 (80/20) powder with Ø = 0.2 mm and (**4**) F1 for comparison.

To improve the catalytic activity, the amount of F2 in the polymer composite was raised from 20 to 35 wt.%. In addition, the polymer composites were modified by reactive extrusion with P(EO-*co*-PO)-NH_2 of different molar masses to enhance the polarity of the polymer matrix, which should improve the distribution of the catalyst particles in the material and hence provide increased accessibility to the active sites. Reactive extrusion of PP-*g*-MA with amines is known to form imide functions in a very fast reaction [35]. Since higher polarity of the polymer matrix could lead to increased leaching, the amino-group-containing ethoxysilane APTES was added during the reactive extrusion process. APTES can, on the one hand, bind to PP-*g*-MA to form the imide. On the other hand, the ethoxysilane groups can react with OH groups remaining in the Fe_2O_3/SiO_x catalyst and can thus generate a chemical linkage between catalyst and polymer matrix. Figure 5 presents the conversion–time curves of the modified polymer composites. All composites caused a linear decrease in RB5 concentration and thus a pseudo-zeroth-order kinetic model (Table 5), indicating the occurrence of a heterogeneous Fenton process. The composites without addition of P(EO-*co*-PO)-NH_2 revealed lower RB5 conversions and lower reaction rate coefficients, suggesting that the accessibility to the active iron oxide particles is more hindered. The addition of APTES resulted in a decrease in conversion and in reaction rate coefficient compared to PP-*g*-MA/F2 (65/35). This could be caused by the covalent attachment of APTES to the polymer matrix and to Fe_2O_3/SiO_x. Increasing molar mass of P(EO-*co*-PO)-NH_2 in the polymer composites enhanced the conversion and reaction rate coefficients of the RB5 degradation. PP-*g*-MA-*g*-PEO1000/APTES/F2 (65/35) exhibited the highest conversion (30%) and reaction rate coefficient (1.03×10^{-9} mol·L^{-1}·s^{-1}).

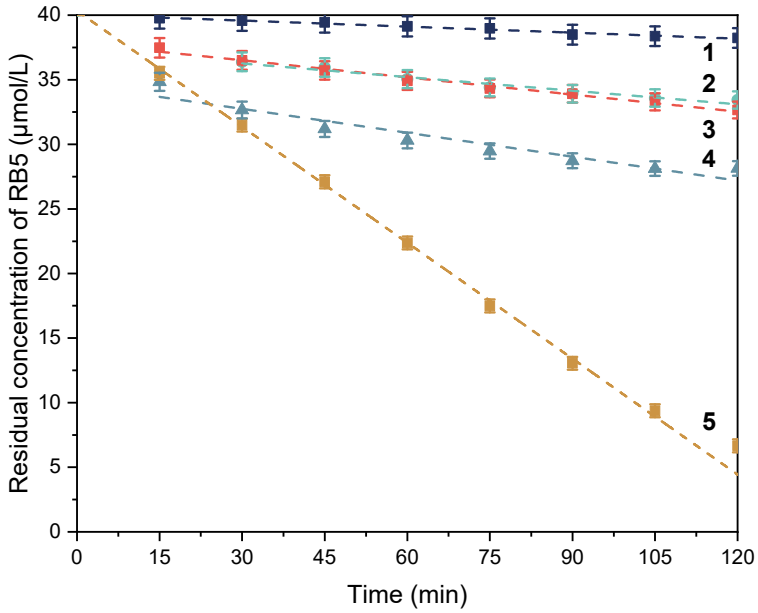

Figure 5. Degradation kinetics of RB5 catalyzed by Fenton polymer composites (**1**) PP-*g*-MA/APTES/F2 (65/35), (**2**) PP-*g*-MA-*g*-PEO600/APTES/F2 (65/35), (**3**) PP-*g*-MA/F2 (65/35), (**4**) PP-*g*-MA-*g*-PEO1000/APTES/F2 (65/35) and (**5**) F2 for comparison.

The composites PP-*g*-MA/F2 (65/35), PP-*g*-MA/APTES/F2 (65/35) and PP-*g*-MA-*g*-PEO600/APTES/F2 (65/35) did not show quantitative iron leaching. Only PP-*g*-MA-*g*-PEO1000/APTES/F2 (65/35) exhibited a weak iron leaching of 0.02%, which represents a 78% reduction compared to F2. The increase in iron concentration during RB5 degradation had no significant influence on the reaction course and coefficient of the polymer composites (see SM, Figure S5), which was taken as further evidence for the pseudo-zeroth-order kinetic model and the homogeneous Fenton catalyst action in the oxidation processes with the polymer composites.

3.2.3. Phenol Degradation Studies Catalyzed by the Fenton Polymer Composites

The polymer composites were also studied to investigate whether they would act as suitable catalysts to degrade phenol. Conditions of phenol degradation were similar to RB5 assay to compare the obtained results. While the RB5 assay reflects the catalytic activity of the catalysts, phenol may be considered as a model substance for degradation of trace substances in wastewater. Figure 6 shows the conversion–time curves of the degradation of phenol in the Fenton processes catalyzed by the Fenton catalysts and the Fenton polymer composites. The degradation of phenol was significantly lower with all Fenton catalysts compared to the conversion of RB5 under the same conditions with the exception of F1. The catalyst F1 caused complete degradation of phenol after 30 min but exhibited the highest iron leaching (3.70 mg/L). Therefore, it can be assumed that the fast degradation of phenol was caused by a predominantly homogeneous process.

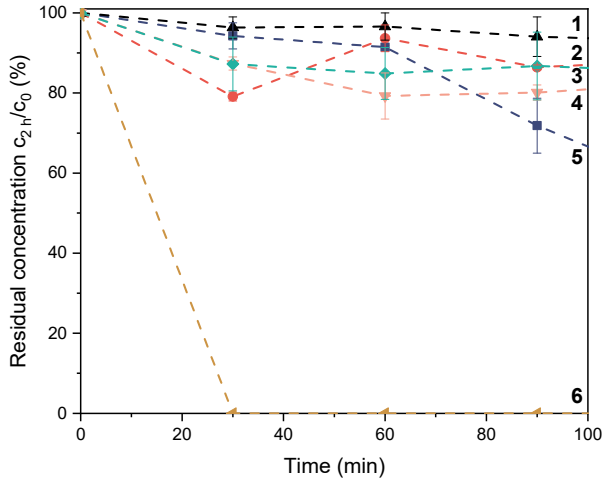

Figure 6. Residual concentration of phenol after 120 min degradation under Fenton conditions catalyzed by (**1**) PP-*g*-MA-g-PEO600/APTES/F2 (65/35) (black line) (**2**) PP-*g*-MA-*g*-PEO1000/APTES/F2 (65/35) (red line), (**3**) F2 (green line), (**4**) PP-*g*-MA/F2 (65/35) (rose line), (**5**) PP-*g*-MA/F1 (80/20) (blue line) and (**6**) F1 (brown line).

After 2 h, 15% of phenol was degraded by F2, while 85% of RB5 was converted. In contrast, the polymer composites, which exhibited much lower conversions for RB5 compared to F2, catalyzed the degradation of phenol with a conversion of 44% for PP-*g*-MA/F1 (80/20), followed by 17% for PP-*g*-MA (65/35), as presented in Table 6. PP-*g*-MA/F1 (80/20) also exhibited the highest iron leaching, being 9 times higher than that for PP-*g*-MA/F2 (65/35), suggesting contributions of homogeneous Fenton processes during phenol degradation. The conversion of phenol with PP-*g*-MA-*g*-PEO1000/APTES/F2 (65/35) was also lower than that with PP-*g*-MA/F2 (65/35), while the former showed a 50% higher conversion in the RB5 assay. The results demonstrate that the two model trace substances examined for degradation are difficult to compare with each other. Obviously, different processes are reflected by the assays. The RB5 assay mostly mirrors the scission of the azo group, while degradation of phenol mostly results in the conversion of phenol in an oligomeric compound [1,17,36] These different processes yielded different activities of the Fenton catalysts.

The iron leaching of all catalysts studied here (F1, F2 and the composites) was significantly lower than found by Botas et al. [37] (11–20 mg/L). Despite higher iron leaching, the phenol conversions found by the authors were lower even though the reaction took place at a higher temperature (80 °C).

Table 6. Conversion of phenol in the Fenton processes catalyzed by the Fenton catalyst F2 and the Fenton polymer composites compared to the iron leaching after 2 h degradation.

Sample	Conversion (%) [(a,b)]	Iron Leaching after 2 h (mg/L) [(a,c)]
F1	100	3.70
F2	15	0.04
PP-*g*-MA/F1 (80/20)	44	0.19
PP-*g*-MA/F2 (65/35)	17	0.04
PP-*g*-MA-*g*-PEO600/APTES/F2 (65/35)	7	0.01
PP-*g*-MA-*g*-PEO1000/APTES/F2 (65/35)	12	0.02

[(a)] The iron content of all samples used was 100 mg/L, [(b)] conversion after 2 h, [(c)] determined by ICP-OES.

3.3. Degradation Studies of Model Substances for Trace Pollutants Catalyzed by F2

The Fenton catalyst F2 was employed to carry out orienting preliminary degradation experiments of organic substances that are considered to be trace pollutants in wastewater. The development of F2 was aimed at applications in a modular two-step system for

wastewater treatment consisting of a Fenton AOP module and a subsequent enzymatic treatment, as reported recently [38]. Therefore, degradation conditions were kept similar to the ones employed before [38], and the same four organic trace compounds were selected for this study. Their chemical structure is illustrated in Figure 7.

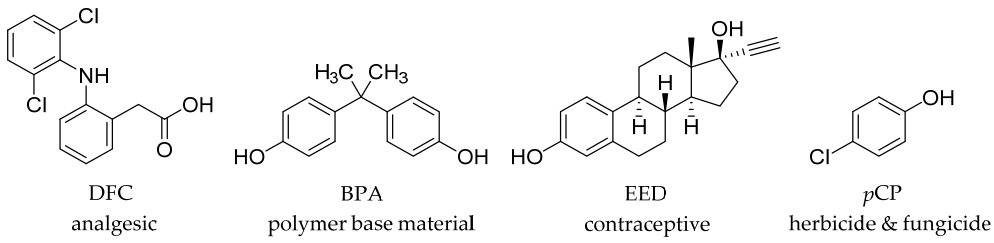

Figure 7. Organic trace pollutants used as model substances for degradation studies with F2.

BPA and *p*CP are phenolic compounds widely used in industry. They cause significant ecotoxicological problems for living organisms [39–42]. Pharmaceuticals such as DFC, a common anti-inflammatory and analgesic drug, and EED, an estrogen drug used in birth control pills, are excreted partially unchanged into the environment and may have toxic effects on aquatic organisms [39,43–45]. While DFC is a carboxylic acid with pKa = 4.15 [46], BPA represents a typical phenol with pKa = 10.3 [46,47]. *p*CP is a chloro-substituted, electron-deficient phenol with pKa = 9.47 [48]. This structure represents a compound that is difficult to oxidize. EED is a phenol substituted by bulky aliphatic cycles terminated by a triple bond with pKa = 10.7 [47]. In this case, the oxidation of the triple bond was expected to occur first and fastly.

The four substances DFC, BPA, EED and *p*CP were tested at a concentration of 10 µM for conversion with the Fenton catalyst F2 in both citrate buffer (pH 4.5) and water (pH 7). The tests in water represent the conditions in water treatment, while pH 4.5 is close to the conditions for standard (homogeneous) Fenton processes.

Figure 8 illustrates the residual concentration of the substances after 24 h of conversion under Fenton conditions.

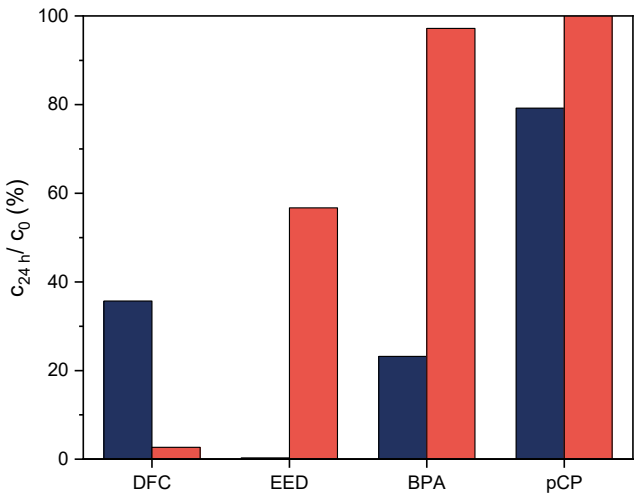

Figure 8. Residual concentration of model substances after 24 h degradation by F2 under Fenton conditions in citrate buffer at pH 4.5 (blue) and water at pH 7 (red).

In citrate buffer, complete degradation of EED (100%), followed by BPA (77%), DFC (64%) and *p*CP (21%) was obtained after 24 h, while in water almost no degradation was observed for *p*CP (0%) and BPA (3%). In contrast, DFC (98%) was almost completely converted in water. The dissociation equilibrium of DFC at pH 7 is shifted to the side of the carboxylate ion, which is more easily oxidizable than the neutral form. BPA, *p*CP and EED possess higher pKa values, indicating that the neutral form is predominant at

pH 7. The enhanced degradation of BPA, *p*CP and EED at lower pH could be attributed to higher iron leaching and thus homogeneous Fenton reaction contributions. In addition, the oxidation potential of the hydroxyl radical increases with lower pH, which also favored the conversion of the trace pollutants. The same trends are reported in the literature [49,50]. The experiments showed the potential of the catalyst studied to degrade these trace substances and the influence of the pH value during the Fenton process.

4. Conclusions

The Fenton catalysts F1 and F2 were successfully synthesized by the sol–gel method and characterized by XRF, XRD and N_2 sorption. The catalytic activity of the catalysts was analyzed by kinetic studies using the RB5 assay in combination with the monitoring of the iron leaching. F1 showed a predominantly homogeneous Fenton reaction with pseudo-first order, while F2 exhibited a pseudo-zeroth order, representing a mainly heterogeneous Fenton catalysis process. This difference was caused by the double calcination procedure applied in the preparation of F2. RB5 was mainly degraded by hydroxyl radicals, as indirectly proven by the addition of radical scavengers.

By mixing these materials in a melt compounding process with modified polypropylene (PP-*g*-MA), the iron leaching was drastically reduced and the reaction became pseudo-zeroth order for all Fenton polymer composites, indicating the occurrence of a heterogeneous Fenton process. Grinding the polymer composites resulted in an increase in the surface area and an enhanced RB5 degradation. PP-*g*-MA-*g*-PEO1000/APTES/F2 (65/35) obtained by reactive extrusion showed the best results in RB5 degradation for the Fenton polymer composite with a conversion of 30% and a low iron leaching of 0.02 wt.% after 2 h.

Phenol degradation studies were additionally carried out for all Fenton catalysts under similar conditions to the RB5 assay. Full conversion, but also the highest iron leaching with >3 wt.%, was reached with F1 after 30 min, proving mainly homogeneous Fenton processes, while PP-*g*-MA/F1 (65/35) revealed the highest phenol degradation (19%) with 0.02 wt.% iron leaching after 2 h.

Initial degradation studies catalyzed by F2 were performed with the model trace compounds DFC, EED, *p*CP and BPA in water at pH 7 and citrate buffer at pH 4.5. The concentration of all substances was measured after performing the Fenton process for 24 h. The highest conversion after 24 h could be reached for EED (100%), followed by DFC (98%).

The experiments showed clearly that iron leaching was almost completely prevented and the Fenton catalysis process proceeded mostly heterogeneously by embedding the silica-supported iron oxide catalysts in polymer matrices. These polymer-embedded heterogeneous catalysts can be prepared in a facile reactive extrusion process, which represents a new concept for the development of heterogeneous Fenton catalysts.

Supplementary Materials: The following are available online at https://www.mdpi.com/article/10.3390/pr9060942/s1, Figure S1: WAXS pattern of the Fenton catalysts F1 and F2 compared to Fe_2O_3 and Fe_3O_4; Figure S2: Adsorption isotherms for N_2 adsorption (filled circles) and desorption (empty circles) of the samples (**1**) F2, (**2**) F1 and (**3**) Fe_2O_3 at 77 K (STP: standard temperature (25 °C) and pressure (100 kPa)); Figure S3: Pore size distribution (PSD) calculated by NLDFT-Fit (cylindrical/sphere pores, adsorption model, N_2 on silica) for F1 (red) and F2 (green); Figure S4: Effect of (a) $O2^{\bullet -}$ scavenger chloroform and (b) $OH^{\bullet}$ scavenger *t*-butanol on the degradation of RB5 catalyzed by the Fenton catalyst F2; Figure S5: Kinetic study of RB5 degradation using the composite PP-*g*-MA-*g*-PEO1000/APTES/F2 (65/35) with different amounts of iron per RB5 assay: (**1**) 100 mg/L iron, (**2**) 200 mg/L iron, (**3**) 300 mg/L iron.

Author Contributions: Conceptualization, D.P., F.M., R.H., P.J.A. and K.L.; methodology, C.H., F.M., D.P., R.H., K.Q., P.J.A. and K.L.; validation, S.I., F.M., K.B.L.B., K.Q., P.J.A. and M.D.; formal analysis, S.I. and M.D.; investigation, C.H., S.I., F.M., K.B.L.B., K.Q., P.J.A. and K.L.; resources, D.P., R.H. and K.L.; data curation, C.H., S.I., D.P. and M.D.; writing—original draft preparation, C.H., S.I., D.P. and K.L.; writing—review and editing, C.H. and D.P.; visualization, C.H., S.I. and M.D.; supervision, D.P., R.H. and K.L.; project administration, D.P., R.H. and K.L.; funding acquisition, D.P., R.H., P.J.A. and

K.L. All authors substantially contributed to the work reported. All authors have read and agreed to the published version of the manuscript.

Funding: German Federal Ministry of Education and Research (BMBF), program KMU-innovativ: Materialforschung (ProMat_KMU), collaboration project CeraFe+ (grant# 13XP5065).

Institutional Review Board Statement: Not applicable.

Informed Consent Statement: Not applicable.

Data Availability Statement: Additional data are given in the Supplementary Material.

Acknowledgments: Financial support by the German Federal Ministry of Education and Research (BMBF) (program KMU-innovativ: Materialforschung (ProMat_KMU)) for the collaboration project CeraFe+ (grant numbers 13XP5065A, 13XP5065B, 13XP5065D, 13XP5065E) is gratefully acknowledged. Furthermore, the authors would like to thank Dipl.-Ing. (FH) Oliver Kobsch for SEM measurements and Dieter Jehnichen, IPF, for kind support during the X-ray measurements.

Conflicts of Interest: The authors declare no conflict of interest.

References

1. Villegas, L.G.C.; Mashhadi, N.; Chen, M.; Mukherjee, D.; Taylor, K.E.; Biswas, N. A Short Review of Techniques for Phenol Removal from Wastewater. *Curr. Pollut. Rep.* **2016**, *2*, 157–167. [CrossRef]
2. Underhill, R.; Lewis, R.J.; Freakley, S.J.; Douthwaite, M.; Miedziak, P.J.; Akdim, O.; Edwards, J.K.; Hutchings, G.J. Oxidative Degradation of Phenol using in situ Generated Hydrogen Peroxide Combined with Fenton's Process. *Johns. Matthey Technol. Rev.* **2018**, *62*, 417–425. [CrossRef]
3. Ni Soon, A.; Hameed, B. Heterogeneous catalytic treatment of synthetic dyes in aqueous media using Fenton and photo-assisted Fenton process. *Desalination* **2011**, *269*, 1–16. [CrossRef]
4. Baptisttella, A.M.S.; de Araujo, C.M.B.; da Silva, M.P.; Nascimento, G.F.O.D.; da Costa, G.R.B.; Nascimento, B.F.D.; Ghislandi, M.G.; Sobrinho, M.A.D.M. Magnetic Fe3O4-graphene oxide nanocomposite—Synthesis and practical application for the heterogeneous photo-Fenton degradation of different dyes in water. *Sep. Sci. Technol.* **2021**, *56*, 425–438. [CrossRef]
5. Lumbaque, E.C.; Gomes, M.F.; Carvalho, V.D.S.; De Freitas, A.M.; Tiburtius, E.R.L. Degradation and ecotoxicity of dye Reactive Black 5 after reductive-oxidative process. *Environ. Sci. Pollut. Res.* **2016**, *24*, 6126–6134. [CrossRef]
6. Kumar, V.; Mohapatra, T.; Dharmadhikari, S.; Ghosh, P. A Review Paper on Heterogeneous Fenton Catalyst: Types of Preparation, Modification Techniques, Factors Affecting the Synthesis, Characterization, and Application in the Wastewater Treatment. *Bull. Chem. React. Eng. Catal.* **2020**, *15*, 1–34. [CrossRef]
7. Buthiyappan, A.; Aziz, A.R.A.; Daud, W.M.A.W. Recent advances and prospects of catalytic advanced oxidation process in treating textile effluents. *Rev. Chem. Eng.* **2016**, *32*, 1–47. [CrossRef]
8. Gaya, U.I.; Abdullah, A.H. Heterogeneous photocatalytic degradation of organic contaminants over titanium dioxide: A review of fundamentals, progress and problems. *J. Photochem. Photobiol. C Photochem. Rev.* **2008**, *9*, 1–12. [CrossRef]
9. Fenton, H.J.H. LXXIII—Oxidation of tartaric acid in presence of iron. *J. Chem. Soc. Trans.* **1894**, *65*, 899–910. [CrossRef]
10. Xu, H.-Y.; Wang, Y.; Shi, T.-N.; He, X.-L.; Qi, S.-Y. Process optimization on methyl orange discoloration in Fe3O4/RGO-H2O2 Fenton-like system. *Water Sci. Technol.* **2018**, *77*, 2929–2939. [CrossRef] [PubMed]
11. Firak, D.S.; Ribeiro, R.R.; De Liz, M.V.; Peralta-Zamora, P. Investigations on iron leaching from oxides and its relevance for radical generation during Fenton-like catalysis. *Environ. Earth Sci.* **2018**, *77*, 117. [CrossRef]
12. Yu, T.; Breslin, C.B. Graphene-Modified Composites and Electrodes and Their Potential Applications in the Electro-Fenton Process. *Materials* **2020**, *13*, 2254. [CrossRef]
13. Fana, X.; Caoa, Q.; Menga, F.; Songa, B.; Baia, Z.; Zhaoa, Y.; Chenab, D.; Zhouc, Y.; Songa, M. A Fenton-like system of biochar loading Fe–Al layered double hydroxides (FeAl-LDH@BC)/H_2O_2 for phenol removal. *Chemosphere* **2021**, *266*, 128992. [CrossRef]
14. Rubeena, K.; Reddy, P.H.P.; Laiju, A.; Nidheesh, P. Iron impregnated biochars as heterogeneous Fenton catalyst for the degradation of acid red 1 dye. *J. Environ. Manag.* **2018**, *226*, 320–328. [CrossRef] [PubMed]
15. Yeh, K.-J.; Chen, T.-C.; Young, W.-L. Competitive Removal of Two Contaminants in a Goethite-Catalyzed Fenton Process at Neutral pH. *Environ. Eng. Sci.* **2013**, *30*, 47–52. [CrossRef]
16. Pradhan, G.K.; Sahu, N.; Parida, K.M. Fabrication of S, N co-doped α-Fe_2O_3 nanostructures: Effect of doping, OH radical formation, surface area, [110] plane and particle size on the photocatalytic activity. *RSC Adv.* **2013**, *3*, 7912–7920. [CrossRef]
17. Jaramillo-Páez, C.; Navío, J.A.; Hidalgo, M.; Bouziani, A.; El Azzouzi, M. Mixed α-Fe_2O_3/Bi_2WO_6 oxides for photoassisted hetero-Fenton degradation of Methyl Orange and Phenol. *J. Photochem. Photobiol. A Chem.* **2017**, *332*, 521–533. [CrossRef]
18. Nguyen, X.S.; Zhang, G.; Yang, X. Mesocrystalline Zn-Doped Fe_3O_4 Hollow Submicrospheres: Formation Mechanism and Enhanced Photo-Fenton Catalytic Performance. *ACS Appl. Mater. Interfaces* **2017**, *9*, 8900–8909. [CrossRef] [PubMed]
19. Arroyo-Gómez, J.; Toncón-Leal, C.; Dos Santos, A.; Moreno, M.; Sapag, K.; Martínez-Huitle, C. Fe/SBA-15: Characterization and its application to a heterogeneous solar photo-Fenton process in order to decolorize and mineralize an azo dye. *Mater. Lett. X* **2020**, *5*, 100034. [CrossRef]

20. Farhadian, N.; Liu, S.; Asadi, A.; Shahlaei, M.; Moradi, S. Enhanced heterogeneous Fenton oxidation of organic pollutant via Fe-containing mesoporous silica composites: A review. *J. Mol. Liq.* **2021**, *321*, 114896. [CrossRef]
21. Sashkina, K.; Parkhomchuk, E.; Rudina, N.; Parmon, V. The role of zeolite Fe-ZSM-5 porous structure for heterogeneous Fenton catalyst activity and stability. *Microporous Mesoporous Mater.* **2014**, *189*, 181–188. [CrossRef]
22. Sashkina, K.A.; Polukhin, A.V.; Labko, V.S.; Ayupov, A.B.; Lysikov, A.I.; Parkhomchuk, E.V. Fe-silicalites as heterogeneous Fenton-type catalysts for radiocobalt removal from EDTA chelates. *Appl. Catal. B Environ.* **2016**, *185*, 353–361. [CrossRef]
23. Calleja, G.; Melero, J.; Martínez, F.; Molina, R. Activity and resistance of iron-containing amorphous, zeolitic and mesostructured materials for wet peroxide oxidation of phenol. *Water Res.* **2005**, *39*, 1741–1750. [CrossRef]
24. Martínez, F.; Molina, R.; Pariente, M.I.; Siles, J.; Melero, J. Low-cost Fe/SiO_2 catalysts for continuous Fenton processes. *Catal. Today* **2017**, *280*, 176–183. [CrossRef]
25. Brunauer, S.; Emmett, P.H.; Teller, E. Adsorption of Gases in Multimolecular Layers. *J. Am. Chem. Soc.* **1938**, *60*, 309–319. [CrossRef]
26. Thommes, M.; Kaneko, K.; Neimark, A.V.; Olivier, J.P.; Rodriguez-Reinoso, F.; Rouquerol, J.; Sing, K.S. Physisorption of gases, with special reference to the evaluation of surface area and pore size distribution (IUPAC Technical Report). *Pure Appl. Chem.* **2015**, *87*, 1051–1069. [CrossRef]
27. Dantas, T.; Mendonça, V.; José, H.; Rodrigues, A.; Moreira, R. Treatment of textile wastewater by heterogeneous Fenton process using a new composite Fe_2O_3/carbon. *Chem. Eng. J.* **2006**, *118*, 77–82. [CrossRef]
28. Martins, R.C.; Lopes, R.J.; Quinta-Ferreira, R.M. Lumped kinetic models for single ozonation of phenolic effluents. *Chem. Eng. J.* **2010**, *165*, 678–685. [CrossRef]
29. Covinich, L.G.; Felissia, F.; Massa, P.; Fenoglio, R.; Area, M.C. Kinetic modeling of a heterogeneous Fenton-type oxidative treatment of complex industrial effluent. *Int. J. Ind. Chem.* **2018**, *9*, 215–229. [CrossRef]
30. Gaya, U.I. *Heterogeneous Photocatalysis Using Inorganic Semiconductor Solids*; Springer Science and Business Media LLC: Berlin/Heidelberg, Germany, 2014.
31. Mitsika, E.E.; Christophoridis, C.; Fytianos, K. Fenton and Fenton-like oxidation of pesticide acetamiprid in water samples: Kinetic study of the degradation and optimization using response surface methodology. *Chemosphere* **2013**, *93*, 1818–1825. [CrossRef]
32. Bae, S.; Kim, D.; Lee, W. Degradation of diclofenac by pyrite catalyzed Fenton oxidation. *Appl. Catal. B Environ.* **2013**, *134–135*, 93–102. [CrossRef]
33. Sun, S.-P.; Lemley, A.T. p-Nitrophenol degradation by a heterogeneous Fenton-like reaction on nano-magnetite: Process optimization, kinetics, and degradation pathways. *J. Mol. Catal. A Chem.* **2011**, *349*, 71–79. [CrossRef]
34. Teel, A.L.; Watts, R.J. Degradation of carbon tetrachloride by modified Fenton's reagent. *J. Hazard. Mater.* **2002**, *94*, 179–189. [CrossRef]
35. Xanthos, M. Interfacial agents for multiphase polymer systems: Recent advances. *Polym. Eng. Sci.* **1988**, *28*, 1392–1400. [CrossRef]
36. Mohammadi, S.; Kargari, A.; Sanaeepur, H.; Abbassian, K.; Najafi, A.; Mofarrah, E. Phenol removal from industrial wastewaters: A short review. *Desalination Water Treat.* **2015**, *53*, 2215–2234. [CrossRef]
37. Botas, J.; Melero, J.; Martínez, F.; Pariente, M.I. Assessment of Fe_2O_3/SiO_2 catalysts for the continuous treatment of phenol aqueous solutions in a fixed bed reactor. *Catal. Today* **2010**, *149*, 334–340. [CrossRef]
38. Horn, C.; Pospiech, D.; Allertz, P.J.; Müller, M.; Salchert, K.; Hommel, R. Chemical Design of Hydrogels with Immobilized Laccase for the Reduction of Persistent Trace Compounds in Wastewater. *ACS Appl. Polym. Mater.* **2021**, *3*, 2823–2834. [CrossRef]
39. Solano, M.D.L.; Montagner, C.C.; Vaccari, C.; Jardim, W.F.; Anselmo-Franci, J.A.; Carolino, R.D.O.; Luvizutto, J.F.; De A Umbuzeiro, G.; De Camargo, J.L. Potential endocrine disruptor activity of drinking water samples. *Endocr. Disruptors* **2015**, *3*, e983384. [CrossRef]
40. Zoeller, R.T.; Brown, T.R.; Doan, L.L.; Gore, A.C.; Skakkebaek, N.E.; Soto, A.M.; Woodruff, T.J.; Saal, F.S.V. Endocrine-Disrupting Chemicals and Public Health Protection: A Statement of Principles from the Endocrine Society. *Endocrinology* **2012**, *153*, 4097–4110. [CrossRef]
41. Olaniran, A.O.; Igbinosa, E. Chlorophenols and other related derivatives of environmental concern: Properties, distribution and microbial degradation processes. *Chemosphere* **2011**, *83*, 1297–1306. [CrossRef]
42. Chen, M.; Xu, P.; Zeng, G.; Yang, C.; Huang, D.; Zhang, J. Bioremediation of soils contaminated with polycyclic aromatic hydrocarbons, petroleum, pesticides, chlorophenols and heavy metals by composting: Applications, microbes and future research needs. *Biotechnol. Adv.* **2015**, *33*, 745–755. [CrossRef] [PubMed]
43. Bonnefille, B.; Gomez, E.; Courant, F.; Escande, A.; Fenet, H. Diclofenac in the marine environment: A review of its occurrence and effects. *Mar. Pollut. Bull.* **2018**, *131*, 496–506. [CrossRef] [PubMed]
44. Gore, A.C.; Crews, D.; Doan, L.L.; La Merrill, M.; Patisaul, H.; Zota, A. *Introduction to Endocrine Disrupting Chemicals (EDCs) A Guide for Public Interest Organizations and Policy-Makers*; Endocrine Society: Washington, DC, USA, 2014; pp. 1–76.
45. Choubert, J.-M.; Ruel, S.M.; Esperanza, M.; Budzinski, H.; Miège, C.; Lagarrigue, C.; Coquery, M. Limiting the emissions of micro-pollutants: What efficiency can we expect from wastewater treatment plants? *Water Sci. Technol.* **2011**, *63*, 57–65. [CrossRef] [PubMed]
46. Margot, J.; Maillard, J.; Rossi, L.; Barry, D.; Holliger, C. Influence of treatment conditions on the oxidation of micropollutants by Trametes versicolor laccase. *New Biotechnol.* **2013**, *30*, 803–813. [CrossRef] [PubMed]

47. Clara, M.; Strenn, B.; Saracevic, E.; Kreuzinger, N. Adsorption of bisphenol-A, 17β-estradiole and 17α-ethinylestradiole to sewage sludge. *Chemosphere* **2004**, *56*, 843–851. [CrossRef]
48. Ding, H.; Li, X.; Wang, J.; Zhang, X.; Chen, C. Adsorption of chlorophenols from aqueous solutions by pristine and surface functionalized single-walled carbon nanotubes. *J. Environ. Sci.* **2016**, *43*, 187–198. [CrossRef]
49. Wang, M.; Fang, G.; Liu, P.; Zhou, D.; Ma, C.; Zhang, D.; Zhan, J. Fe_3O_4@β-CD nanocomposite as heterogeneous Fenton-like catalyst for enhanced degradation of 4-chlorophenol (4-CP). *Appl. Catal. B Environ.* **2016**, *188*, 113–122. [CrossRef]
50. Huang, R.; Fang, Z.; Yan, X.; Cheng, W. Heterogeneous sono-Fenton catalytic degradation of bisphenol A by Fe3O4 magnetic nanoparticles under neutral condition. *Chem. Eng. J.* **2012**, *197*, 242–249. [CrossRef]